

## Formation and properties of metal–oxygen atomic chains

This content has been downloaded from IOPscience. Please scroll down to see the full text.

2008 New J. Phys. 10 033005

(<http://iopscience.iop.org/1367-2630/10/3/033005>)

View [the table of contents for this issue](#), or go to the [journal homepage](#) for more

Download details:

IP Address: 132.229.211.17

This content was downloaded on 10/05/2017 at 12:23

Please note that [terms and conditions apply](#).

You may also be interested in:

[Metallic properties of magnesium point contacts](#)

R H M Smit, A I Mares, M Häfner et al.

[The high-bias stability of monatomic chains](#)

R H M Smit, C Untiedt and J M van Ruitenbeek

[Mechanically controllable bi-stable states in a highly conductive single pyrazine molecular junction](#)

Satoshi Kaneko, Carlo Motta, Gian Paolo Brivio et al.

[Point-contact spectroscopy on aluminium atomic-size contacts: longitudinal and transverse vibronic excitations](#)

T Böhler, A Edtbauer and E Scheer

[Single-atom contacts with a scanning tunnelling microscope](#)

J Kröger, N Néel, A Sperl et al.

[Charge transport through molecular switches](#)

Sense Jan van der

Molen and Peter Liljeroth

[Spin fluctuation effects on the conductance through a single Pd atom contact](#)

M A Romero, S C Gómez-Carrillo, P G Bolcatto et al.

[Electronic and atomic shell structure in aluminium nanowires](#)

A I Mares, D F Urban, J Bürki et al.

[The effect of bonding of a CO molecule on the conductance of atomic metal wires](#)

M Kiguchi, D Djukic and J M van Ruitenbeek

## Formation and properties of metal–oxygen atomic chains

W H A Thijssen<sup>1</sup>, M Strange<sup>2</sup>, J M J aan de Brugh<sup>2,3</sup>  
and J M van Ruitenbeek<sup>1,4</sup>

<sup>1</sup> Kamerlingh Onnes Laboratory, Leiden University, P O Box 9504, 2300 RA Leiden, The Netherlands

<sup>2</sup> Center for Atomic-Scale Materials Physics, Department of Physics, Technical University of Denmark, DK-2800 Lyngby, Denmark

<sup>3</sup> Solid State Physics Group, MESA+ Research Institute, University of Twente, P O Box 217, 7500 AE Enschede, The Netherlands

E-mail: [Ruitenbeek@physics.leidenuniv.nl](mailto:Ruitenbeek@physics.leidenuniv.nl)

*New Journal of Physics* **10** (2008) 033005 (16pp)

Received 22 September 2007

Published 4 March 2008

Online at <http://www.njp.org/>

doi:10.1088/1367-2630/10/3/033005

**Abstract.** Suspended chains consisting of single noble metal and oxygen atoms have been formed. We provide evidence that oxygen can react with and be incorporated into metallic one-dimensional atomic chains. Oxygen incorporation reinforces the linear bonds in the chain, which facilitates the creation of longer atomic chains. The mechanical and electrical properties of these diatomic chains have been investigated by determining local vibration modes of the chain and by measuring the dependence of the average chain-conductance on the length of the chain. Additionally, we have performed calculations that give insight into the physical mechanism of the oxygen-induced strengthening of the linear bonds and the conductance of the metal–oxygen chains.

<sup>4</sup> Author to whom any correspondence should be addressed.

**Contents**

<b>1. Introduction</b>	<b>2</b>
<b>2. Experimental technique</b>	<b>3</b>
<b>3. Observation of oxygen induced atomic chains</b>	<b>3</b>
<b>4. Point contact spectroscopy on metal–oxygen chains</b>	<b>9</b>
<b>5. Calculations</b>	<b>11</b>
<b>6. Conclusion</b>	<b>15</b>
<b>Acknowledgment</b>	<b>15</b>
<b>References</b>	<b>15</b>

**1. Introduction**

Freely suspended atomically thin metallic wires are the ultimate one-dimensional (1D) conductors. Since their discovery [1, 2], scientists have been amazed by the mere existence of these wires, since at first one would not expect such 1D structures to be able to physically exist: the capillary instability that is also observed when droplets break off a forming water column would destroy the one-dimensionality since the surface tension is not strong enough to keep the structure together. In fact, atomic wires are only observed when they are suspended between metal electrodes at both sides or supported by a substrate on which they can be artificially created atom by atom [3, 4] or formed by self-assembly [5]. Once the wire breaks due to a critical build-up of stress in the chain, the atoms collapse back to the electrode since the necessary wire tension that kept the structure together has disappeared. Atomic wires have actually only been observed for the three 5d transition metals Au, Pt and Ir in break-junction experiments at low temperatures [6], although there is evidence for the formation of short chains for silver [7] and alloys [8] in TEM experiments at room temperature in ultra high vacuum (UHV). It has been argued that the physical mechanism that drives atomic chain formation is similar to what drives spontaneous surface reconstructions in these same metals, a delicate balance between the s and d electron density of states influenced by relativistic effects [9, 10]. Due to the high charge of the nucleus the lowest s-electron orbitals become relativistically contracted, which causes a lowering of the Fermi energy resulting in a small depletion of the anti-bonding states in the d-band. In the case of the 5d transition metals this relativistic effect is large enough to tip the energy balance for the formation of surface reconstructions and the formation of atomic chains. This is not the case for 4d and 3d transition metals [6]. Indeed a Ag(110) surface does not form a missing row reconstruction while Au(110) does.

Experimentally freely suspended atomic wires can be created by means of the mechanically controlled break junction (MCBJ) technique [11], which is employed in this work. With this technique a small junction can be mechanically broken and be brought into contact again. Alternative approaches involve the use of a STM, the tip of which can be contacted with a surface [12] or by creating holes in a thin metallic foil by electron bombardment until a single strand of gold atoms is left, which can be imaged by TEM [2, 13]. The MCBJ technique and the electron bombardment technique have shown a large discrepancy in the observed interatomic distances between the atoms in the chain. For a gold chain created by the MCBJ technique in cryogenic vacuum an interatomic distance of  $2.5 \pm 0.2 \text{ \AA}$  is observed [14] while

room temperature TEM images give distances up to 4 Å [2, 13]. Based on model calculations, it has been suggested that these large interatomic distances are due to the incorporation of foreign atoms like oxygen [15], hydrogen [16], carbon or nitrogen [17, 18] that are not resolved by TEM (with the possible exception of [19]). Oxygen is an especially interesting candidate since density functional theory (DFT) calculations have shown that the total energy of a gold atomic chain with atomic oxygen incorporated is lowered compared to clean gold [15] and the Au–O bond is able to sustain higher pulling forces before breaking [20]. We have previously given experimental evidence showing that oxygen can indeed be incorporated into atomic gold chains and that oxygen induces chain formation for silver, which is known not to form chains in pure form [21]. In this paper, we will provide further evidence for oxygen incorporation by demonstrating the presence of oxygen in the chain by local vibration-mode spectroscopy and by calculations on the conductance properties of the chains, which strongly support our experimental observations.

## 2. Experimental technique

In our experiments we used poly-crystalline Au, Ag and Cu wires with a diameter of 100  $\mu\text{m}$  and a purity of 99.999%. After creating a circular notch in the middle of the wire, it is fixed on a bendable substrate in a three-point bending configuration. By using a mechanical axle the wire can be broken and with a piezoelectric element it is possible to control the distance between the two electrodes with atomic precision. A detailed description of the MBCJ technique can be found in [22]. Our experiments were performed in cryogenic vacuum. Once the sample chamber is evacuated and cooled down to 5 K the wire is broken for the first time ensuring clean fracture surfaces. Close to the junction a local heater and thermometer are mounted, which enable us to control the temperature of the junction between 5 and 60 K, while the vacuum can remain at 5 K. In order to be able to admit oxygen to the junction the insert is equipped with a capillary attached to a high purity oxygen reservoir. To prevent premature condensation of oxygen, the capillary has a heating wire running all along the interior. To prevent other molecules from entering into the sample chamber while admitting oxygen through the heated capillary, it is pumped and baked out by means of the heating wire at 150 °C, prior to the cool down. Two point conductance measurements are performed to determine the conductance of the atomic wires. Differential conductance ( $dI/dV$ ) measurements were performed on the atomic wires using a lock-in amplifier. The bias voltage was modulated with a fixed modulation amplitude of 1 mV and a frequency of 7 kHz, while sweeping the dc bias voltage from +100 to –100 mV and back.

## 3. Observation of oxygen induced atomic chains

Microscopic junctions of gold, silver and copper are carefully broken and the conductance is observed to decrease stepwise until finally the contact has a cross-section equal to the diameter of only a single atom. For the noble metals the conductance of single-atom contacts is close to one quantum unit of conductance,  $G_0 = 2e^2 h^{-1}$ . For gold it is known that upon stretching a single atom contact, additional atoms can be pulled out of the electrodes to form a monatomic chain of up to seven atoms long [1, 23, 24]. This manifests itself in long plateaus with conductances around  $1 G_0$  that are observed while monitoring the conductance of gold contacts as they are pulled apart. Such long plateaus are not observed for silver and copper as

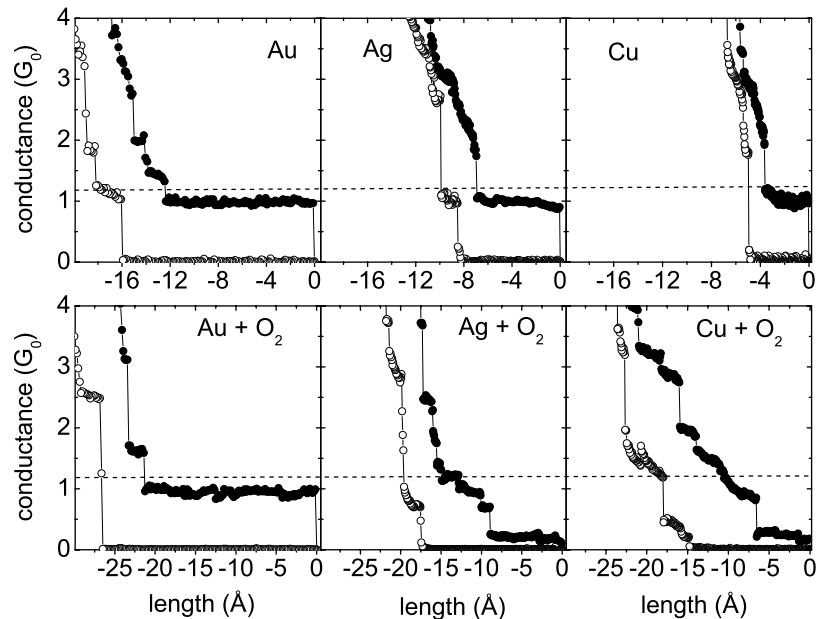


**Figure 1.** Typical conductance traces for gold, silver and copper with and without oxygen admitted. The filled dots show the digitalized points measured while breaking the contact, while the open dots are measured when closing the junction again.

can be seen in figure 1. This indicates that silver and copper do not form long single atom wires like gold does.

When oxygen is admitted to the contact and the temperature is kept at 5 K, interesting differences in the conductances and lengths of the last plateaus are observed: in the case of gold the conductance and the average length of the chains do not change noticeably. This is in contrast to what is seen in the case of the non-chain-forming metals silver and copper. The conductance of the last plateau drops sharply towards 0.1 and 0.2  $G_0$  for silver and copper, respectively, and the average total length increases dramatically. Only when the temperature of the gold sample is increased to about 40 K does the average chain length also increase. One way to obtain more quantitative information about the conductance of the atomic contacts and chains is to record conductance histograms. By recording all conductances that are measured when a contact is being pulled apart and plotting them in a histogram, a conductance histogram is obtained. After breaking and measuring many junctions the preferential conductances can be determined. In figure 2, conductance histograms for the three noble metals are shown with and without oxygen admitted. In order to focus on the changes that occur due to the admission of oxygen, the histograms have been normalized to the area under the curves. For the clean metals one can clearly see that a peak near 1  $G_0$  is dominant over all other conductances. When oxygen is introduced the dominant peak at 1  $G_0$  decreases sharply for silver and copper due to a shift of weight to lower conductance values. For gold at 5 K no significant changes are seen as was discussed above. These observations indicate that oxygen influences the atomic contacts of silver and copper in such a way that configurations with conductances near 1  $G_0$  are less frequently obtained. The conductance of atomic contacts for gold is apparently hardly influenced by oxygen since the conductance histograms of figure 2 are nearly identical.

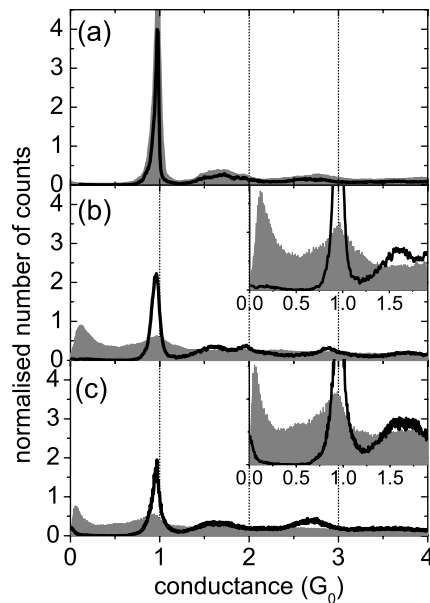


**Figure 2.** Conductance histograms for Au (a), Ag (b) and Cu (c) without (black curves) and with oxygen admitted (filled graphs). For clarity the histograms have been normalized to the area under the curves. Each histogram is constructed from the digitalized points (filled dots of figure 1) obtained from approximately 2000 curves recorded at a bias voltage of 50 mV at  $T = 5$  K.

Recently, we have presented evidence [21] that Au atomic wires become reinforced and therefore can be stretched to longer lengths as a result of their reaction with oxygen at 40 K. Furthermore, we have shown that this bond strengthening effect is even more pronounced for silver wires. We have studied the chain formation process under the influence of oxygen for the three noble metals. Since the conductance of an atomic chain or single-atom contact of noble metals are known to be close to  $1 G_0$  we can measure the lengths of a large ensemble of conductance plateaus near  $1 G_0$  and construct a length histogram. In such a histogram the lengths of the plateaus are plotted against the number of times those lengths were observed. It can be clearly seen from the conductance histograms of figure 2 that in the case of silver and copper with oxygen admitted a large portion of the observed conductances have values below  $1 G_0$ . We suspect that these low conductance values belong to silver and copper atomic wires that are influenced by oxygen and therefore we have included these conductances in the chain length measurements. The length of the chains is obtained by measuring the distance which the electrodes move apart from the moment when the conductance of the contact drops below  $1.1 G_0$ , until it drops below  $0.05 G_0$ . In the case of gold a conductance limit of  $0.5 G_0$  was used for stopping the chain length measurement.

In figures 3 (a), (c) and (e), the length histograms for the three clean noble metals and those with oxygen admitted are shown. What is immediately seen is that the average chain length for all three metals increases upon oxygen admission. This effect is clearly the strongest for the non-chain-forming metals silver and copper. In all length histograms one can clearly see a number of more or less equidistant peaks. For silver–oxygen and copper–oxygen chains the distances between the peaks are about  $1.5 \pm 0.2$  and  $1.2 \pm 0.2$  Å, respectively. These equidistant peaks

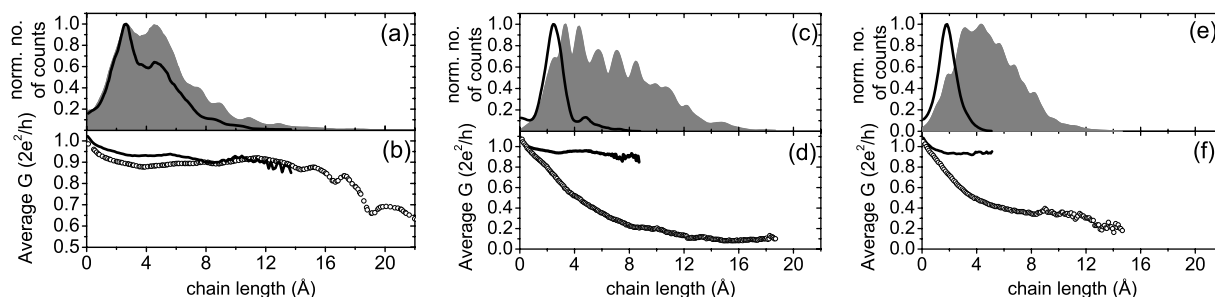


**Figure 3.** Length histograms of stretch distances for contacts with conductance near  $1 G_0$  and lower of Au (a), Ag (c) and Cu (e) in pure form (black curves) and with oxygen admitted (filled graphs). For the pure metals the lengths were measured in a conductance window of  $G \in [1.1, 0.5]$ , while with oxygen admitted  $G \in [1.1, 0.05]$ . The lower panels show the average conductance as a function of stretch distance for clean Au (b), Ag (d) and Cu (f) (black curves) and with oxygen admitted (open dots). All data were obtained with a bias voltage of 50 mV. The temperature for graphs (a) and (b) was 40 K and for (c)–(f) 5 K.

give a strong indication of atomic chains being formed and the distances between the peaks have previously been interpreted as the interatomic distance in the chains [1]. When assuming that oxygen is indeed taken up in the atomic chain structure, the interpretation of the peak structure in terms of bond lengths for such a diatomic chain is less straight forward. A bond length of only  $1.2 \text{ \AA}$  is not expected and is about 60% smaller than for the gold–oxygen chains (see figure 3(a)). DFT calculations have predicted bond lengths of  $1.9$  and  $1.8 \text{ \AA}$  for silver–oxygen and copper–oxygen chains, respectively [25]. The shoulder to the left of the silver–oxygen length histogram of figure 3 is located at the same position as the dominant peak in the clean silver histogram. Therefore, it is most probably caused by the rupture of a  $>\text{Ag}-\text{Ag}<$  contact, with  $>$  and  $<$  denoting the connections to the left and right electrodes. We will discuss our interpretation of the peak positions that arise in the length histograms of figure 3(c) below.

A length count is taken at the moment an atomic chain breaks and the atoms collapse back to the electrodes, which causes the conductance of the junction to drop deep into the tunneling regime. A rupture can occur when one of the linear 1D bonds cannot be stretched any further due to a critical build-up of energy in the chain. But sometimes it is possible that an additional atom, which is weakly bound to the bulk atoms at one of the electrode apexes, is pulled into the atomic chain. Consequently, the chain remains intact and the tension of the linear bonds is relaxed. Then it is possible to stretch the 1D structure further until again a critical build-up of energy occurs, which can result in rupture or the elongation of the chain with yet another atom. This sequence repeats itself over and over again and the incorporation of atoms will stop when the supply of loosely bound atoms at the apexes of the electrodes is depleted. The peaks in the length histograms indicate lengths at which there is a higher preference for the atomic chain to break and therefore represent atomic chain lengths in a stretched configuration.

From the length histogram of clean Ag in figure 3, we obtain a Ag–Ag bond length of  $2.4 \text{ \AA}$ . In order to simplify the analysis, we assume that the bond length at the edges where the atomic chain is contacted to the electrodes with either a Ag or an O atom is comparable. For the Ag–O bond length, we take the calculated value of  $1.8 \pm 0.1 \text{ \AA}$  [25, 26]. With these ingredients we are able to identify chain compositions consisting of Ag and O atoms for which

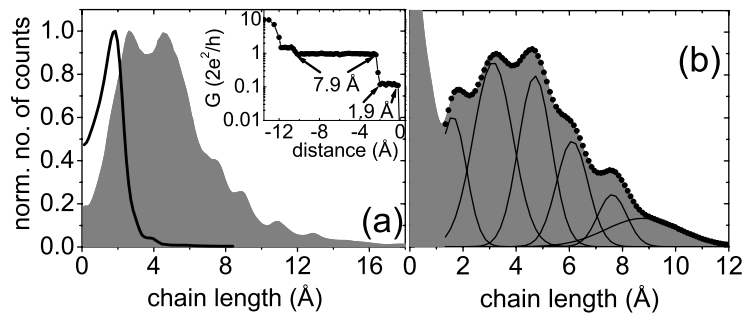


**Figure 4.** (a) Length histogram for Au–O chains at 40 K with conductance limits between  $1.1$  and  $0.5 G_0$  (filled graph) compared to a length histogram with conductance limits between  $0.2$  and  $0.05 G_0$  (black curve). (b) Length histogram of Ag–O chains at 5 K with conductance values between  $0.5$  and  $0.05 G_0$ . All histograms were taken at a bias voltage of 50 mV and consist of at least 2000 traces.

the lengths fit the peak positions in the length histogram of figure 3. The peak distance in this interpretation is the result of various combinations of Ag–Ag and Ag–O bond lengths. There are typically several chain compositions that result in a similar chain length. Although most peak positions can be accommodated in this scheme there are a few compositions that do not fit any of the peak positions in the length histogram. Possibly, the number of O atoms available, or the dynamics of chain formation, restrict the accessible chain configurations. A similar analysis can be made for the peak positions of the Cu–O length histogram of figure 3(e), which yields a Cu–O bond of  $1.7 \pm 0.1 \text{ \AA}$ . We are aware that this analysis relies on a few simplifying assumptions. Our main message is that the peak distance in the histograms cannot be interpreted directly as the metal–oxygen bond distance, but that such peak structure arises naturally from the various combinations of atoms composing the chains.

The decrease of the conductance of the chains as the chains become longer is very nicely seen in figures 3(b), (d) and (f). While for silver–oxygen and copper–oxygen chains the drop in conductance starts already for relatively short chains, gold–oxygen chains display a lower conductance only when they are on average longer than about 16 Å, corresponding to a chain with a length of more than six gold atoms. Indeed for Au–O chains created at 40 K it is sometimes observed that upon stretching the conductance makes a sudden jump from a value around  $1 G_0$  to about  $0.1 G_0$  as can be seen in the inset of figure 4(a). We have investigated these lower conduction plateaus by recording a length histogram between conductance values of  $0.2$  and  $0.05 G_0$ . In figure 4(a), the length histogram for low conductance values of Au–O chains is shown. It is dominated by a single peak at 1.9 Å. A second small peak can be seen at 3.9 Å. This distance is the same as the Au–O distance that we observed in the length histogram of figure 3(a). Furthermore it is striking that plateaus at  $0.1 G_0$  are typically only one bond length long and only occur when a chain of certain length has already been formed.

We conclude, therefore, that the atomic unit that is being pulled into the chain and causes the sharp drop in conductance, also destabilizes the chain since upon further pulling the chain breaks in nearly all cases. The plateaus at  $0.1 G_0$  have only been seen at temperatures  $\geq 40 \text{ K}$ . The higher mobility and vapor pressure of oxygen molecules at those temperatures increases the supply of oxygen molecules around the region where the chain is formed. We speculate that

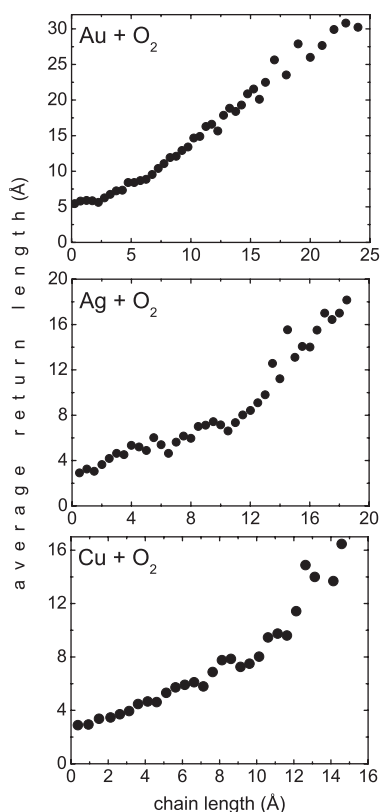


**Figure 5.** Average return lengths as a function of atomic chain length for Au (a), Ag (b) and Cu (c) with admitted oxygen at, respectively, 40, 5 and 5 K.

the low conductance plateau is caused by the appearance of oxygen–oxygen bonds in the chain which could severely lower both the conductance and the bond strength.

A length histogram obtained for low-conductance silver–oxygen chain structures is shown in figure 4(b). In contrast to gold (figure 4(a)) chain formation continues by incorporating more atomic units into the chain since multiple peaks in the length histogram are observed. The inter-peak distance is  $1.5 \pm 0.2 \text{ \AA}$ , which is the same as in the histogram of figure 3(c), indicating that both silver and oxygen atoms are being pulled into the chain.

More evidence to support that freely suspended long atomic wires are being formed of gold, silver and copper with chemisorbed oxygen incorporated comes from the dependence of the average return length on the chain length. When an atomic wire is formed, atoms are pulled out of the electrodes in order to be incorporated into the atomic wire upon stretching the contact. When a wire breaks, the atoms collapse back to the electrodes and the conductance drops deep into the vacuum tunneling regime. We then reverse the direction of movement of the electrodes towards each other. At the moment that mechanical contact is remade the conductance jumps from a value in the tunneling regime to a value of the order of  $1 G_0$ . By measuring this so-called return length for every wire that is broken we obtain the average return length for a given atomic chain length. Figure 5 shows the average return length for gold–oxygen, silver–oxygen and copper–oxygen chains. In all cases, an offset is observed followed by an increase in average return length as a function of chain length. The offset indicates that even for a single atom contact that breaks before forming a chain the electrodes move back a certain distance. This is

due to the fact that the single atom connects the two electrodes and it can sustain a force upon pulling on it. This causes a counter-force pulling on the electrodes, which will slightly elastically deform them. When the contact breaks the stress can be released and the atoms relax and move back into their equilibrium position. But when longer chains are being formed and eventually broken the atoms that made up the chain collapse back to the electrodes and consequently the electrodes have to move back a longer distance upon increasing chain length. Given the fact that the average return length increases more or less linearly with chain length we have a strong indication that atomic chains of noble metal atoms with oxygen are indeed being formed. The deviation from a purely linear increase could be the result of a larger energy stored in the longer chains, because more metal oxygen bonds are present that can sustain higher pulling forces. When such long chains break the stored elastic energy may propel atoms away from the junction area. The force a silver–oxygen bond in an infinite alternating silver–oxygen chain can sustain is about 2.4 times larger than for a silver–silver bond in a infinite silver chain [25]. Meanwhile the difference in the case of pure gold and gold–oxygen is about a factor 1.5 [15, 20] explaining why this effect does not appear so clearly in gold–oxygen return lengths.

#### 4. Point contact spectroscopy on metal–oxygen chains

In the previous section, we have provided evidence that oxygen can chemically react with noble metal contacts or chains and reinforce the linear bonds in the wires so that they can be elongated further. In this section, we present evidence that oxygen most probably is dissociated and incorporated into the atomic chains as is predicted by DFT model calculations [15, 20].

We have verified the incorporation of oxygen by point contact spectroscopy. This technique forms a powerful tool for studying the interactions of electrons with vibrational excitations in a metallic contact [27, 28]. An atomic chain of noble metal atoms is a ballistic conductor for low bias voltages, since it has one nearly completely transparent conductance channel resulting in a total conductance very close to  $1 G_0$  [29]–[31]. However, electrons with sufficient energy have a small probability to excite phonon modes in an atomic chain and by means of differential conductance ( $dI/dV$ ) spectroscopy the energies for those modes can be determined as was shown for clean gold atomic wires [32]. About 1% of all forward traveling electrons with an excess energy larger than the energy of a phonon mode actually do excite such a mode. Those electrons lose energy, which forces them to scatter back since all forward moving states below  $E_F + eV_{\text{bias}}$  are already occupied for a perfect single-channel conductor. This backscattering causes a small decrease of the total conductance of the atomic chain. The observation of this small signal is often hampered by conductance fluctuations, which result from interference of electron trajectories scattering off defects near the contact [33, 34]. In the case of the *s*-like noble metals that have a nearly 100% transparent single channel these conductance fluctuations are strongly suppressed [33]. From figure 3, we see that gold–oxygen chains have a conductance that is close to  $1 G_0$  and we have observed phonon modes for medium-length gold–oxygen wires. Differential conductance spectra were recorded by keeping the atomic chain at a fixed elongation and measuring the current modulation as was described before. Figure 6 displays two spectra that were obtained for 7 Å long gold–oxygen wires at 5 K. Clearly two downward steps at different voltages in each spectrum can be seen, indicating a possible onset of phonon excitations at those energies. The low-energy phonon mode has an energy at  $17 \pm 2$  meV in figures 6(a) and  $15 \pm 2$  meV in (b). The high-energy mode that is observed has an energy of

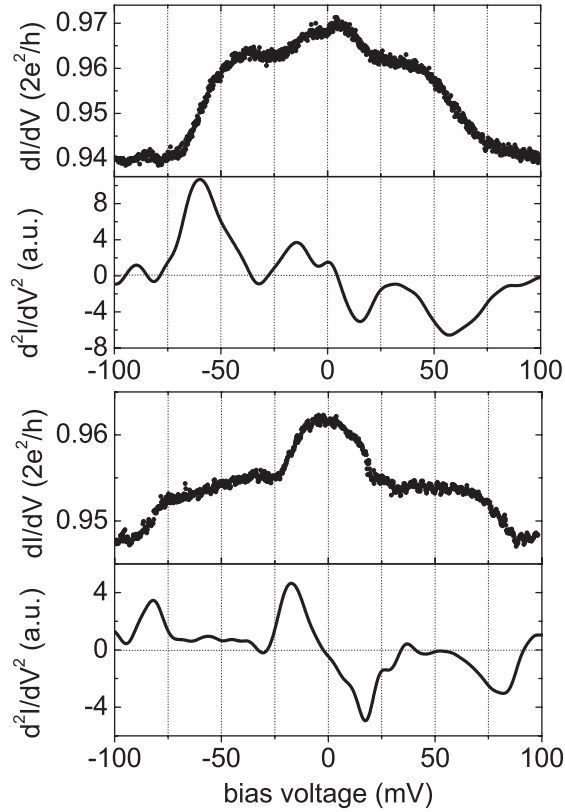


**Figure 6.** Two typical differential conductance spectra taken for Au atomic chains after admitting oxygen at 4.2 K. The chains were pulled to a length of about 7 Å.

$82 \pm 4$  and  $60 \pm 4$  meV in figures 6(a) and (b), respectively. All spectra that we have observed, which display two phonon steps, have high-energy modes between 60 and 80 meV.

In order to give a qualitative explanation of the observed vibration mode energies, let us take a look at a simple classical spring–mass model. The model consists of two gold atoms attached to solid walls and an oxygen atom connected by springs in between the gold atoms. We consider only the longitudinal eigenfrequencies, because the probability of exciting transversal modes is very small given the quasi 1D geometry of the atomic chain. By solving the equations of motion, we obtain three frequencies for masses  $M$  and  $m$  for gold and oxygen, respectively. Here, we have used similar spring constants  $k$  between all masses for simplicity, and obtain

$$\begin{aligned}\omega_1^2 &= \frac{M+m-\sqrt{M^2+m^2}}{Mm}k, \\ \omega_2^2 &= \frac{2}{M}k, \\ \omega_3^2 &= \frac{M+m+\sqrt{M^2+m^2}}{Mm}k.\end{aligned}\tag{1}$$

The lowest frequency mode  $\omega_1$  corresponds to the in-phase motion of all atoms. In the second mode  $\omega_2$  the oxygen atom is immobile and the gold atoms move in anti-phase. The highest frequency mode  $\omega_3$  corresponds to the oxygen atom moving in anti-phase with the

gold atoms. By substituting the masses for gold and oxygen atoms, we find that the ratio of two low-energy modes  $\omega_1$  and  $\omega_2$  is 1.4. The heavy-mass modes will be close to the energy of the longitudinal mode for clean atomic gold chains, that are found at about 10–15 meV depending on stretching [32]. From equation (1) the high-energy mode can then be expected at  $65 \pm 10$  meV. Preliminary DFT calculations on gold–oxygen chains predict a high energy mode in the range of 60–80 meV [26], depending on the stress in the linear bonds. Figure 6 shows a high-energy mode at 60 meV and one at 80 meV, comfortably in the range of our simple model and the preliminary calculations. Note that, while the differences in energy seen in figure 6 may come from activation of different vibration modes, differences in the composition of the atomic chains may also lead to variations in the observed vibration energy.

Additionally, our analysis of the gold–oxygen vibration modes provides evidence that oxygen atoms, rather than molecules, are incorporated in atomic chains having a conductance close to  $1 G_0$ : an oxygen molecule has double the mass of an atom, which would shift the energy of the vibration mode down by a factor  $\sqrt{2}$  to  $46 \pm 7$  meV, assuming a similar bond strength to gold, clearly different from the experimental values.

We also performed point contact spectroscopy on silver–oxygen atomic chains. In contrast to the gold–oxygen atomic chains, the conductance of the silver–oxygen chains is typically much lower than  $1 G_0$ , which indicates that the conductance is not made up from a single fully transparent conduction channel. Normally, when one deals with one or more partly opened conduction channels the  $dI/dV$  spectrum is dominated by conductance fluctuations [34]. This makes the observation of steps in  $dI/dV$  due to inelastic scattering of electrons on local vibration-modes very difficult. Furthermore it was recently claimed that the inelastic correction to the conductance changes from a negative contribution for a single conduction channel with  $G > 0.5 G_0$  to positive for  $G < 0.5 G_0$  [35]–[37]. We obtained a few spectra for silver–oxygen chains with a conductance  $\leq 0.5 G_0$ , which displayed bias-symmetric step-like features at energies far above 20 meV (see figure 7).

One can distinguish clearly a step-like increase of the conductance around 80 and 100 meV for the top and bottom spectra, respectively, which would indicate forward scattered inelastic electrons, in agreement with theory [37]. The energies of 80–100 meV are in the range where local vibration modes of these 1D structures can be expected, albeit that compared to the 60–80 meV for the gold–oxygen chains they are somewhat high. Since the energy is far above the Debye energy for silver, the modes are related to incorporated oxygen in the chain.

## 5. Calculations

In this section, we present DFT calculations for the conductance, bonding properties and vibrational properties of Ag–O contacts. Electronic structure calculations are performed using a plane wave implementation of DFT [38]. Exchange and correlation effects are treated at the generalized gradient approximation (GGA) level using the PW91 energy functional [39] and the nuclei and core electrons are described by ultrasoft pseudopotentials [40]. The Kohn Sham (KS) eigenstates are expanded in plane waves with a kinetic energy less than 400 eV. The width of the Fermi–Dirac distribution for occupation numbers is set to 0.1 eV and the total energies are extrapolated to  $T = 0$ .

We first consider a linear Ag chain with an interatomic distance of 2.6 Å and a linear alternating Ag–O chain with an interatomic distance of 2.0 Å. The supercell for the chains has transverse dimensions  $12 \times 12$  Å and we align the chains to the  $z$ -direction. The band structure

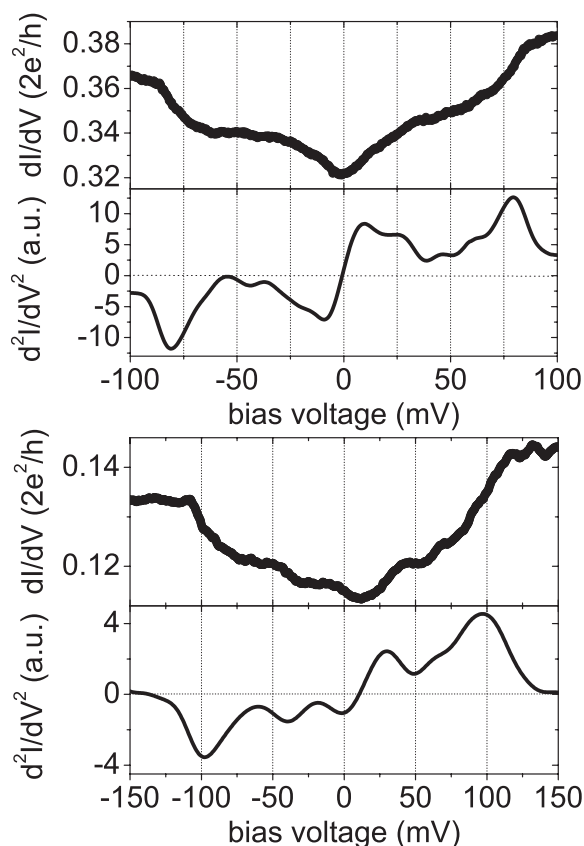


**Figure 7.** Two  $dI/dV$  spectra taken for Ag atomic chains after admitting oxygen at 5 K. The top spectrum was obtained for a chain of about 7 Å in length and the bottom graph for an 11 Å long chain. The  $d^2I/dV^2$  spectra have been smoothed for clarity.

for Ag and Ag–O chains are shown in figure 8 in the upper and lower graph, respectively. The dashed lines indicate slightly strained chains, with the interatomic distance increased by 0.2 Å. The Ag chain is not magnetic and has fully occupied 4d bands and a half filled 5s band. For the Ag–O chain we find a magnetic moment of  $1.0\mu_B$  per Ag–O atom unit and the energy gain, due to the spin-polarization is 0.12 eV per Ag–O atom unit.

The bands for the Ag–O chain can be grouped according to the angular momentum quanta,  $m$ , in the chain direction. The two lowest lying bands are the spin-split O-2s ( $m = 0$ ) bands. The remaining bands shown are Ag-4d bands ( $m = \pm 2$ ) and Ag-4d–O-2p hybrid bands ( $m = 0, \pm 1$ ). Straining the Ag–O chain changes the profile of all bands (dashed lines). However, only two of the spin bands with d–p character change considerably indicating that these bands are relevant for the covalent bonding between Ag and O. The two bands are singly degenerate since they have  $m = 0$  and correspond to a  $d_{z^2}$ – $p_z$  hybrid band with bonding character. Novaes *et al* [20] recently showed that the covalent bond between Au and O is mainly due to the bonding state between Au-5 $d_{z^2}$  and O-2 $p_z$ , in agreement with our findings. It has been argued before that an interesting connection exists between the observation of surface reconstructions and the atomic chain formation in the metals gold, platinum and iridium [6]. In this context, it is remarkable that oxygen-induced surface reconstructions on Ag(110) and Cu(110) have been observed [41, 42],

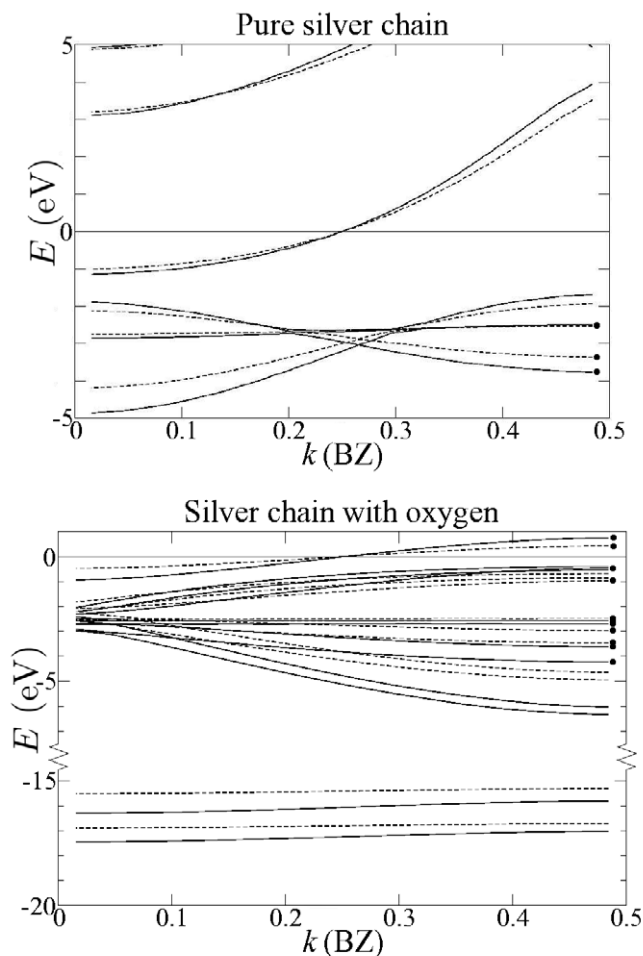


**Figure 8.** Upper graph: band structure for an infinite pure silver chain with an interatomic distance of 2.6 Å (continuous lines) and 2.8 Å (dashed lines). No spin-polarization. Lower graph: band structure of an infinite alternating silver–oxygen chain with an interatomic distance of 2.0 Å (continuous lines) and 2.2 Å (dashed lines). Bands are split into spin up and spin down bands and degenerate bands are marked with a dot. In both cases, 32  $k$ -points are used for the whole Brillouin zone.

while we here provide experimental evidence for atomic chain formation for these metals upon oxygen chemisorption. Therefore, we suspect that the oxygen chemisorption on metal surfaces and the consequent reconstruction originates from the d–p hybrid bands playing the same role as the d-bands in the chain forming metals.

There is a doubly degenerate spin band crossing the Fermi level in figure 8 with  $m = \pm 1$ , i.e. a  $d_{xy}$ – $p_x$  band and a  $d_{yz}$ – $p_y$  band. This shows that magnetic Ag–O chains are metallic and can support two spin channels for a total maximum conductance of  $1 G_0$ . However, our experiments show that finite Ag–O chains often display conductances considerably below  $1 G_0$ .

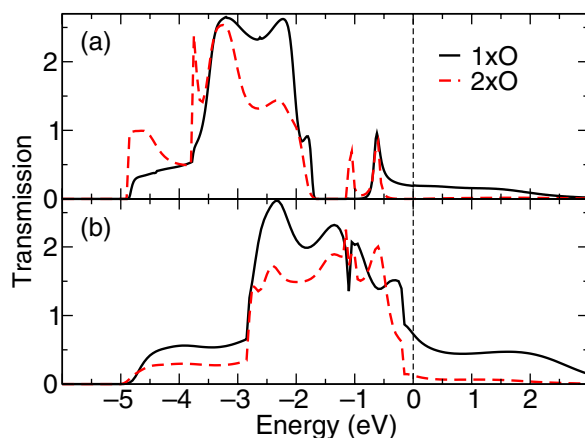


**Figure 9.** (a) Transmission function for a  $\text{Ag-O}$  (full curve) and  $\text{Ag-O-Ag-O}$  (dashed curve) wire contacted by semi-infinite silver atomic wires. (b) Transmission function for a  $\text{Au-O}$  (full curve) and  $\text{Au-O-Au-O}$  (dashed curve) wire contacted by semi-infinite gold atomic wires.

To investigate this, we have calculated the spin-paired transmission function for finite  $\text{Ag-O}$  wires with semi-infinite silver chains as leads. For comparison we have also performed calculations with gold instead of silver. We use a Green's function method for phase coherent electron transport, where both the Green's function of the semi-infinite leads and the scattering region are evaluated in terms of consisting of maximally localized Wannier functions [43].

Figures 9(a) and (b) show the transmission functions for finite  $\text{Ag-O}$  and  $\text{Au-O}$  wires sandwiched between Ag and Au chains, respectively. The full line is for a  $\text{Ag/Au-O}$  wire sandwiched between leads and the dashed line is for a  $\text{Ag/Au-O-Ag/Au-O}$  wire between the leads. The Fermi level is at zero and is indicated by the vertical dashed line.

The transmission function for  $\text{Ag-O}$  displays one eigenchannel in the energy range  $-2$  to  $3$  eV, indicating that the eigenchannel state has  $m = 0$ . The only available state on the O atom with  $m = 0$  in the relevant energy range is the  $2p_z$ , which is then the current carrying state on the O atom. This is confirmed by the projected density of states for  $\text{O-}2p_z$  (not shown), showing the resonance in the transmission function below the Fermi level originating from an anti-bonding combination of the  $\text{O-}2p_z$  orbital and the  $\text{Ag-d}_{z^2}$  band in the leads. The broadening of the resonance is due to the coupling to the s-band in Ag. The bonding combination falls outside the Ag lead bands and is a bound state. In the case of  $\text{Ag-O-Ag-O}$  units, the two resonances have a similar origin, but the transmission at the Fermi level is reduced considerably.

The transmission function for the  $\text{Au-O}$  system shown in figure 9(b) consists of a single eigenchannel with  $m = 0$ , in the energy range from  $-0.15$ – $3.0$  eV. Below  $-0.15$  eV, there are Au d-bands with  $m = \pm 1$  which can couple to O  $m = \pm 1$  states. This results in two extra eigenchannels making the  $2p_z$  resonance less visible except for the tail starting at  $-0.15$  eV and extending to  $3$  eV.

As seen in figures 9(a) and (b), an oxygen atom scatters more strongly electrons around the Fermi level in the  $m = 0$  channel in the case of Ag than for Au. This is in agreement with our experiments, as we observed in figure 3, a tendency for  $\text{Ag-O}$  chains to have a lower conductance than  $\text{Au-O}$  chains. However, in a more realistic contact with surface electrodes as leads, we suspect a finite coupling between  $m = \pm 1$  finite  $\text{d-}2p$  hybrid chain states and

the d states in the metal electrodes, which would result in a higher conductance. A conductance calculation on Ag–O chains involving more realistic electrodes will be published elsewhere.

We also studied the longitudinal vibration-mode energies of a single oxygen atom in a silver contact, we define a supercell with  $3 \times 3$  atoms in the surface plane and which contains 7 atomic layers. The oxygen atom is clamped between two 4 atom pyramids pointing in opposite directions and is attached to Ag (111) surfaces. The Ag (111) surfaces are separated by  $12.7 \text{ \AA}$ . We use a  $4 \times 4$   $k$ -point Monkhorstpack mesh in the surface Brillouin zone. The two pyramids and the oxygen atom were relaxed, until the total residual force was below  $0.05 \text{ eV \AA}^{-1}$ . The calculated longitudinal vibrational mode energies for the two apex silver atoms and the oxygen atom are:  $\omega_1 = 81.4$ ,  $\omega_2 = 28.5$  and  $\omega_3 = 14.7 \text{ meV}$ . The three vibrational modes correspond to: (i) the oxygen atom moving in anti-phase with the silver atoms. (ii) The two Ag atoms moving in anti-phase and the oxygen atom being immobile. (iii) In phase motion of all three atoms.

The relation between the vibration-mode energies can be accounted for by a simple model as described in the previous section and we indeed see that the value of the calculated high-energy mode is in good agreement, with the measured vibrational energies in the range 80–100 meV, indicating that single oxygen atoms are indeed incorporated in the chains.

Recently, Ishida [44] presented calculations for chains of Au and Ag atoms with a single O atom inserted. Ishida's results also show a high transmission at the Fermi energy for oxygen in Au chains, although for a single O atom it has more the character of a resonance. For Ag the conductance is more strongly suppressed.

## 6. Conclusion

We have studied the effects of oxygen on the atomic chain formation for the noble metals gold, silver and copper. By studying the conductance and mechanical properties of these atomic chains, we provided evidence that oxygen atoms can be incorporated in atomic chains. While atomic gold chains retain a conductance near  $1 G_0$  when oxygen is incorporated, the conductance is much reduced for silver and copper chains that form upon chemisorption of oxygen atoms. The increased linear bond strength makes it possible to form silver–oxygen and copper–oxygen atomic chains. Our analysis of the interatomic distances in the silver–oxygen and copper–oxygen chains has indicated the presence of metal–oxygen bonds in the chain. The point contact spectra obtained on the metal–oxygen chains give additional evidence that atomic (not molecular) oxygen is incorporated in the atomic chains. The observation that oxygen can be incorporated in atomic chains and thereby increase the linear bond strength could open possibilities for other molecules to be incorporated in atomic chains. This could lead to interesting new physical properties of these ultimate 1D structures.

## Acknowledgment

This work is part of the research program of the 'Stichting FOM', which is financially supported by NWO.

## References

- [1] Yanson A I, Rubio Bollinger G, van den Brom H E, Agrait N and van Ruitenbeek J M 1998 *Nature* **395** 783
- [2] Ohnishi H, Kondo Y and Takayanagi K 1998 *Nature* **395** 780

- [3] Nilius N, Wallis T M and Ho W 2002 *Science* **297** 1853
- [4] Wallis T M, Nilius N and Ho W 2002 *Phys. Rev. Lett.* **89** 236802
- [5] Gurlu O, Adam O A O, Zandvliet H J W and Poelsema B 2003 *Appl. Phys. Lett.* **83** 4610
- [6] Smit R H M, Untiedt C, Yanson A I and van Ruitenbeek J M 2001 *Phys. Rev. Lett.* **87** 266102
- [7] Rodrigues V, Bettini J, Rocha A R, Rego L G C and Ugarte D 2002 *Phys. Rev. B* **65** 153402
- [8] Bettini J, Sato F, Coura P Z, Dantas S O, Galvão D S and Ugarte D 2006 *Nat. Nanotechnol.* **1** 182
- [9] Takeuchi N, Chan C T and Ho K M 1989 *Phys. Rev. Lett.* **63** 1273  
Takeuchi N, Chan C T and Ho K M 1991 *Phys. Rev. B* **43** 14363
- [10] Pyykkö P 1988 *Chem. Rev.* **88** 563
- [11] Muller C J, van Ruitenbeek J M and de Jongh L J 1992 *Phys. Rev. Lett.* **69** 140
- [12] Agraït N, Rodrigo J G and Vieira S 1993 *Phys. Rev. B* **47** R12345
- [13] Rodrigues V and Ugarte D 2001 *Phys. Rev. B* **63** 073405
- [14] Untiedt C, Yanson A I, Grande R, Rubio Bollinger G, Agraït N, Vieira S and van Ruitenbeek J M 2002 *Phys. Rev. B* **66** 085418
- [15] Bahn S R, Lopez N, Nørskov J K and Jacobsen K W 2002 *Phys. Rev. B* **66** 081405
- [16] Skorodumova N V and Simak S I 2003 *Phys. Rev. B* **67** 121404
- [17] Legoas S B, Galvão D S, Rodrigues V and Ugarte D 2002 *Phys. Rev. Lett.* **88** 076105
- [18] Novaes F D, da Silva A J R, da Silva E Z and Fazzio A 2003 *Phys. Rev. Lett.* **90** 036101
- [19] Legoas S B, Rodrigues V, Ugarte D and Galvão D S 2005 *Phys. Rev. Lett.* **95** 169602
- [20] Novaes F D, da Silva A J R, da Silva E Z and Fazzio A 2006 *Phys. Rev. Lett.* **96** 016104
- [21] Thijssen W H A, Marjenburgh D, Bremmer R H and van Ruitenbeek J M 2006 *Phys. Rev. Lett.* **96** 026806
- [22] Agraït N, Levy Yeyati A and van Ruitenbeek J M 2003 *Phys. Rep.* **377** 81
- [23] Hakkinen H, Barnett R N, Scherbakov A G and Landman U 2000 *J. Chem. Phys. B* **104** 9063
- [24] Bahn S R and Jacobsen K W 2001 *Phys. Rev. Lett.* **87** 266101
- [25] Aan de Brugh J M J 2005 *Master Thesis* Technical University of Denmark
- [26] da Silva A J R 2006 private communication
- [27] Yanson I K and Shklyarevskii O I 1986 *Sov. J. Low Temp. Phys.* **12** 509
- [28] Khotkevich A V and Yanson I K 1995 *Atlas of Point Contact Spectra of Electron–Phonon Interactions in Metals* (Dordrecht: Kluwer)
- [29] Scheer E, Agraït N, Cuevas J C, Levy Yeyati A, Ludoph B, Martín-Rodero A, Rubio Bollinger G, van Ruitenbeek J M and Urbina C 1998 *Nature* **394** 154
- [30] van den Brom H E and van Ruitenbeek J M 1999 *Phys. Rev. Lett.* **82** 1526
- [31] Scheer E, Belzig W, Naveh Y, Devoret M H, Esteve D and Urbina C 2001 *Phys. Rev. Lett.* **86** 284
- [32] Agraït N, Untiedt C, Rubio Bollinger G and Vieira S 2002 *Phys. Rev. Lett.* **88** 216803
- [33] Ludoph B, Devoret M H, Esteve D, Urbina C and van Ruitenbeek J M 1999 *Phys. Rev. Lett.* **82** 1530
- [34] Ludoph and van Ruitenbeek J M 2000 *Phys. Rev. B* **61** 2273
- [35] Viljas J K, Cuevas J C, Pauly F and Häfner M 2005 *Phys. Rev. B* **72** 245415
- [36] Paulsson M, Frederiksen T and Brandbyge M 2005 *Phys. Rev. B* **72** 201101
- [37] de la Vega L, Martín-Rodero A, Agraït N and Levy Yeyati A 2006 *Phys. Rev. B* **73** 075428
- [38] Kohn W and Sham L J 1965 *Phys. Rev. A* **140** 1133
- [39] Perdew J P, Chevary J A, Vosko S H, Jackson K A, Pederson M R, Singh D J and Fiolhais C 1992 *Phys. Rev. B* **46** 6671
- [40] Vanderbilt D 1990 *Phys. Rev. B* **41** R7892
- [41] Taniguchi M, Tanaka K, Hashizume T and Sakurai T 1992 *Surf. Sci. Lett.* **262** L123
- [42] Besenbacher F and Nørskov J K 1993 *Prog. Surf. Sci.* **44** 5
- [43] Thygesen K S and Jacobsen K W 2006 *Chem. Phys.* **319** 111
- [44] Ishida H 2007 *Phys. Rev. B* **75** 205419